Fig. DR1. Geological profiles with sample locations of the black shale-hosted Úrkút Mn-carbonate deposit. Sampling 2009, Úrkút Mine, Shaft No. III, deep level, +180 m; total No. of samples 112 spanning 917 cm from the base to the top of the three ore layers and the intervening black shale. Key: fragm-fragmented sample; cont.-continuous sampling; not cont.-not continuous sampling; numbers on the stratigraphic columns are sample numbers; * indicates samples for XRD; 0 indicates samples for thin sections (in brackets the number of thin sections, total 90); Profiles 1, 3, 4, 5 are from main ore bed, Profile Za and Zb are from second ore bed. Patterns show only color varieties and not sedimentary structures.

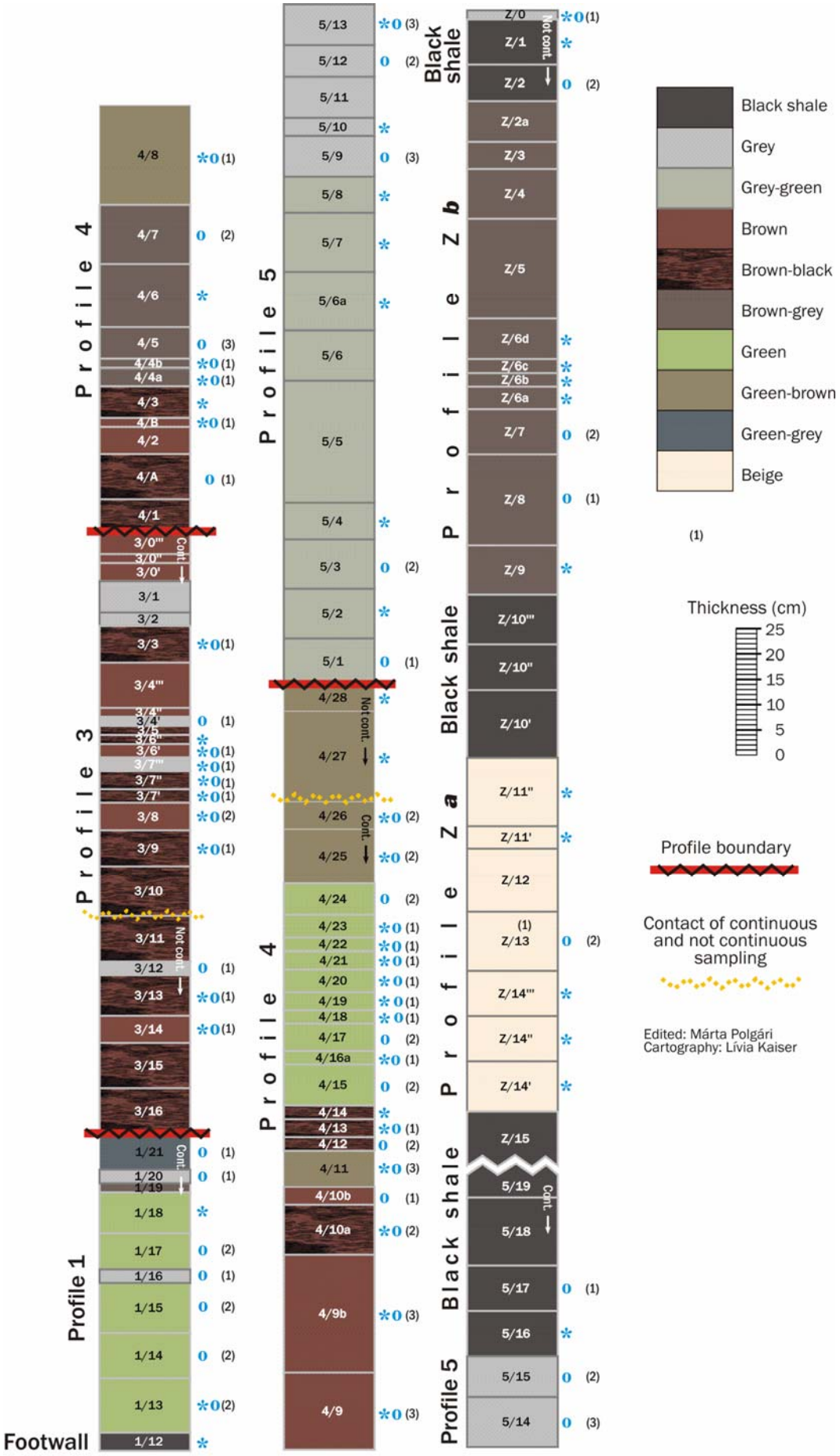

Fig. DR2. Thin section photos showing Fe-rich biomat structures for different representative samples and magnifications. The thickness of the thin sections and the density of biomats are variable. Arrows show representative parts of mineralized filamentous structures. For sample locations see Fig. DR1. Ninety thin section were studied. (Thin sections by Alexandra Müller, IGR, Budapest and TU, Freiberg).

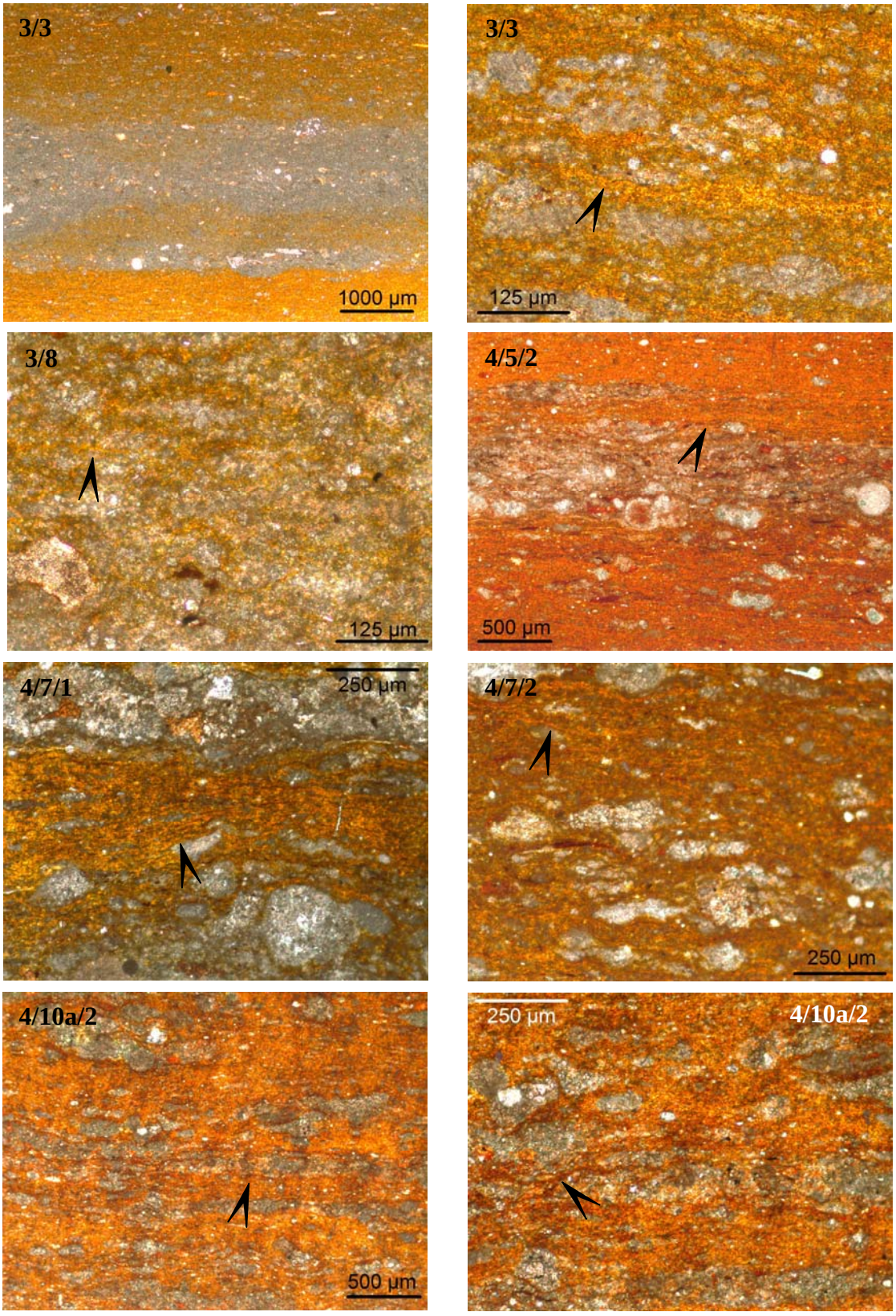

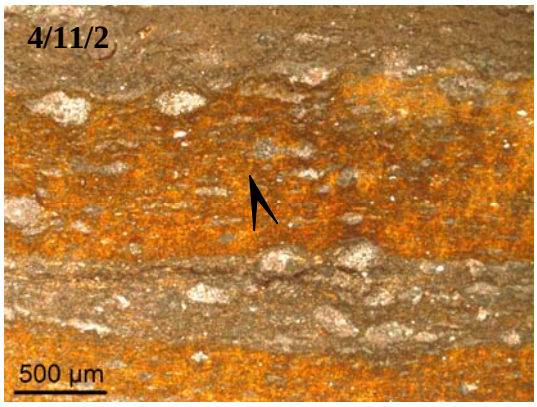
4/11/2
500 µm

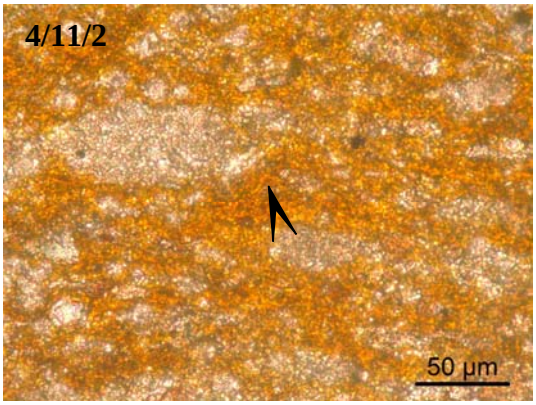
4/11/2
50 µm

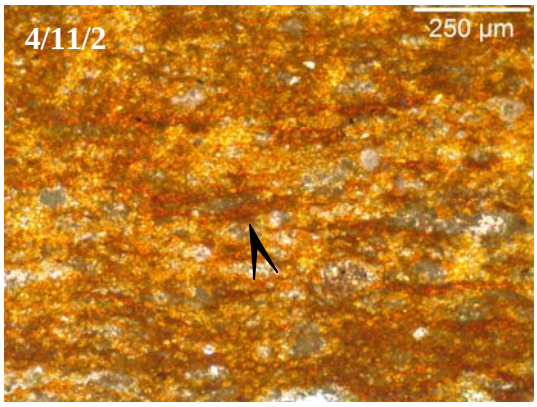
4/11/2
250 µm

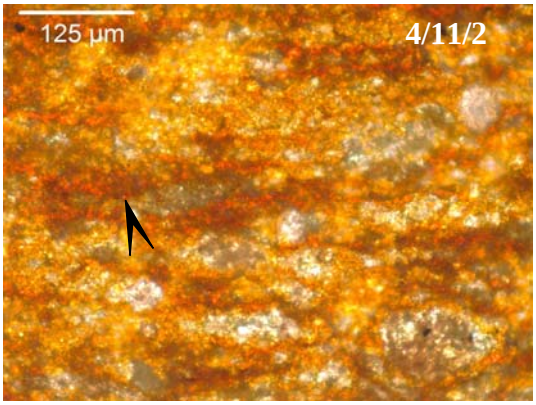
125 µm
4/11/2

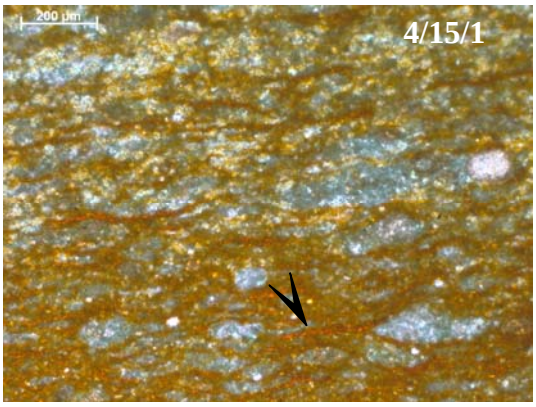
200 µm
4/15/1

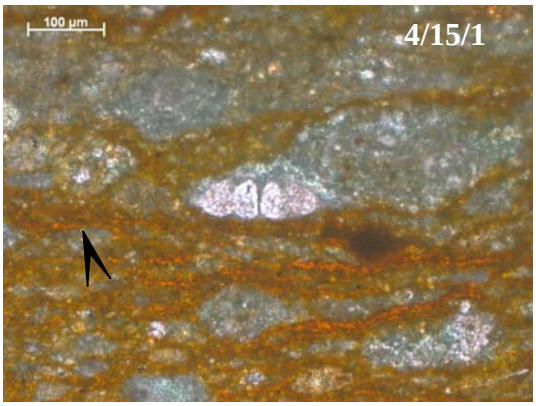
100 µm
4/15/1

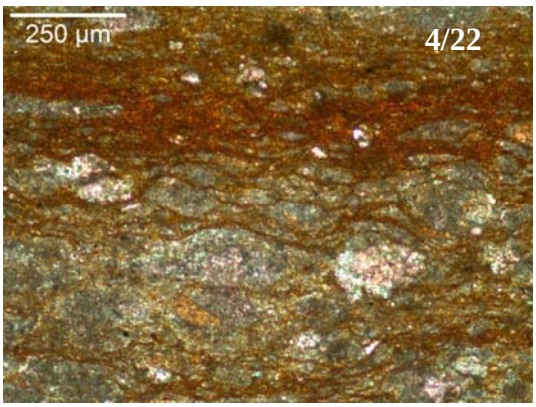
250 µm
4/22

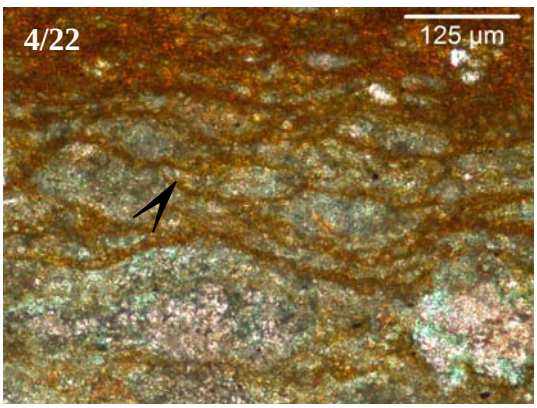
4/22
125 µm

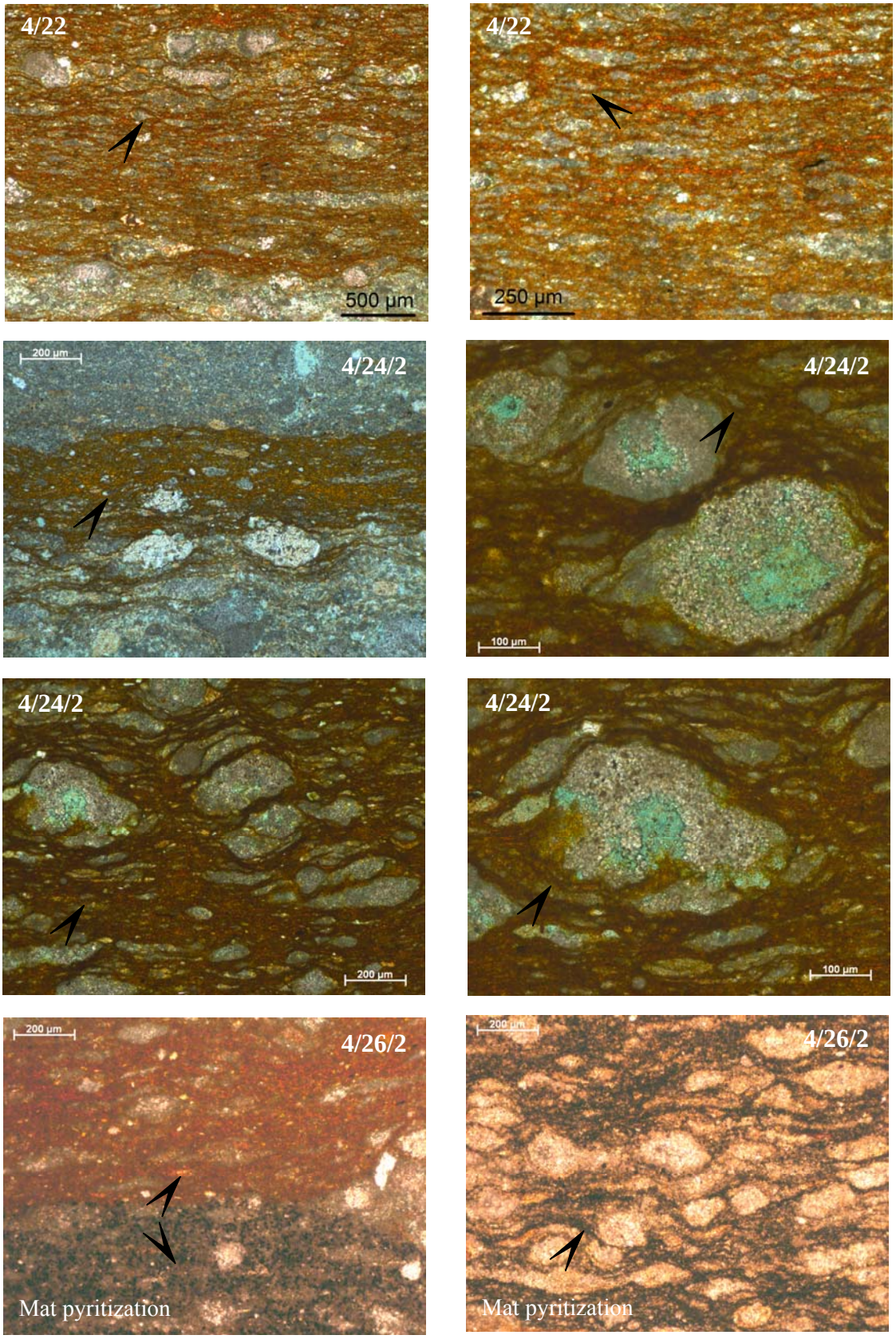

Note - Microbial population growth phases: *lag phase:* bacteria adapt themselves to growth conditions, it is the period where the individual bacteria are maturing and not yet able to divide, synthesis of enzymes and other molecules occurs; *log phase:* a period characterized by cell doubling, the number of new bacteria appearing per unit time is proportional to the present population called the logarithmic phase, with exponential growth; *stationary (stat) phase:* the growth rate slows as a result of nutrient depletion and accumulation of toxic products, this phase is reached as the bacteria begin to exhaust the resources that are available to them, this phase is a constant value as the rate of bacterial growth is equal to the rate of bacterial death; *decline (dec) phase:* closes the growth period (exponential death phase), nutrients in the external environment remain limited or the quantities become exceeding low, bacteria succumb to their own wastes (but endospores survive). Source: http://en.wikipedia.org/wiki/Bacterial_growth

Fig. DR3. Mineral composition (XRD) of Mn-carbonate ore samples and macroscopically separated subsamples normalized to 100% (for sample locations see Fig. DR1)

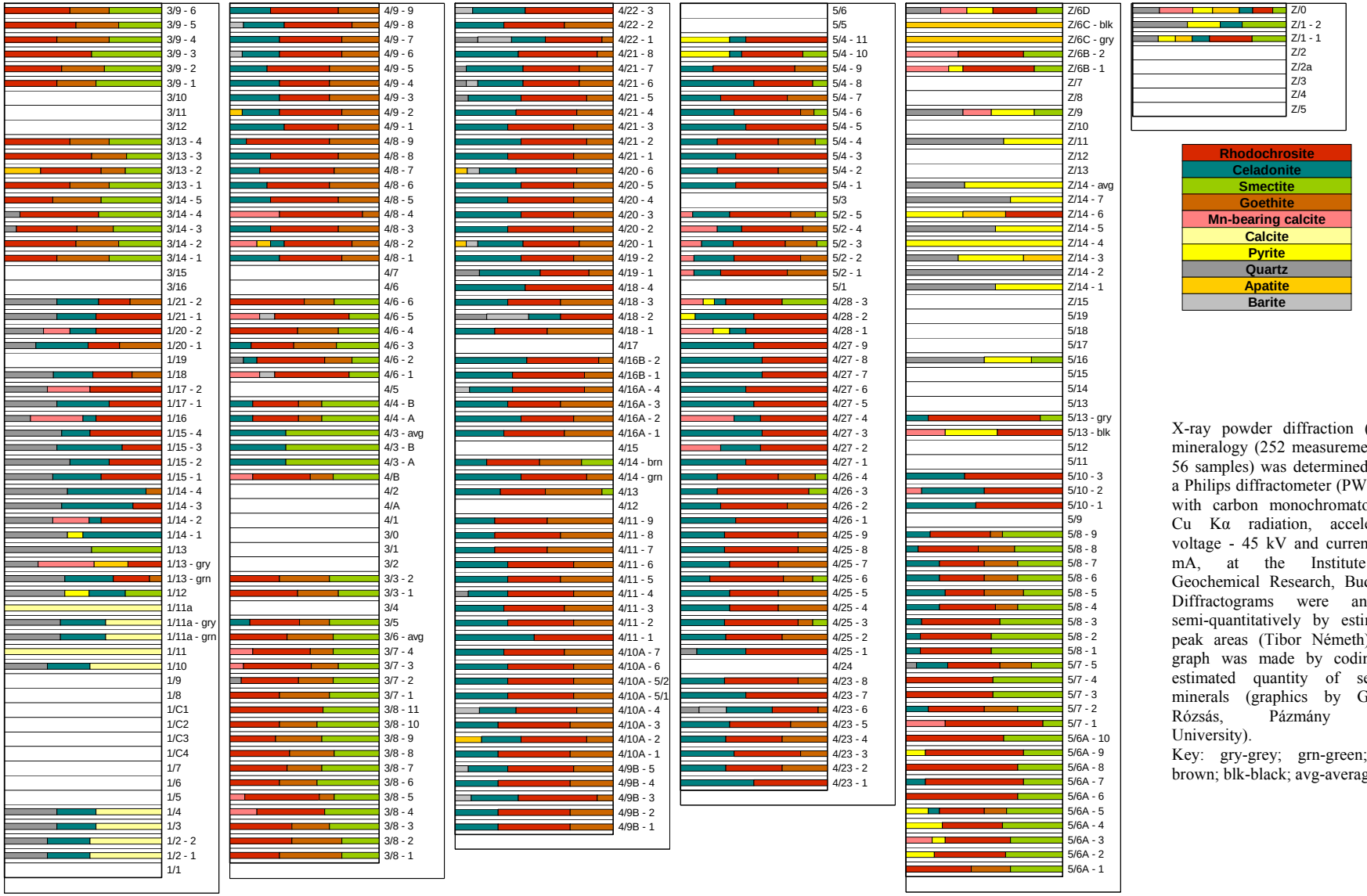

X-ray powder diffraction (XRD) mineralogy (252 measurements on 56 samples) was determined using a Philips diffractometer (PW 1710) with carbon monochromator and Cu Kα radiation, accelerating voltage - 45 kV and current - 35 mA, at the Institute for Geochemical Research, Budapest. Diffractograms were analyzed semi-quantitatively by estimating peak areas (Tibor Németh). The graph was made by coding the estimated quantity of selected minerals (graphics by Gergely Rózsás, Pázmány Péter University).

Key: gry-grey; grn-green; brn-brown; blk-black; avg-average

Fig. DR4. Composite image of 4/25 thin section with bands (1-3) of Raman microscopy measurements and series of Raman spectra acquired along a vertical section indicated on the oriented thin section (arrow points to top of section). On sections numbering 1 to 3, plus marks (+) on the columns with numbers off to the side indicate the points where Raman spectra were acquired. Distance between two measured points is equal to 250 μm. Fig. 1. includes section with spectra No. 93-103.

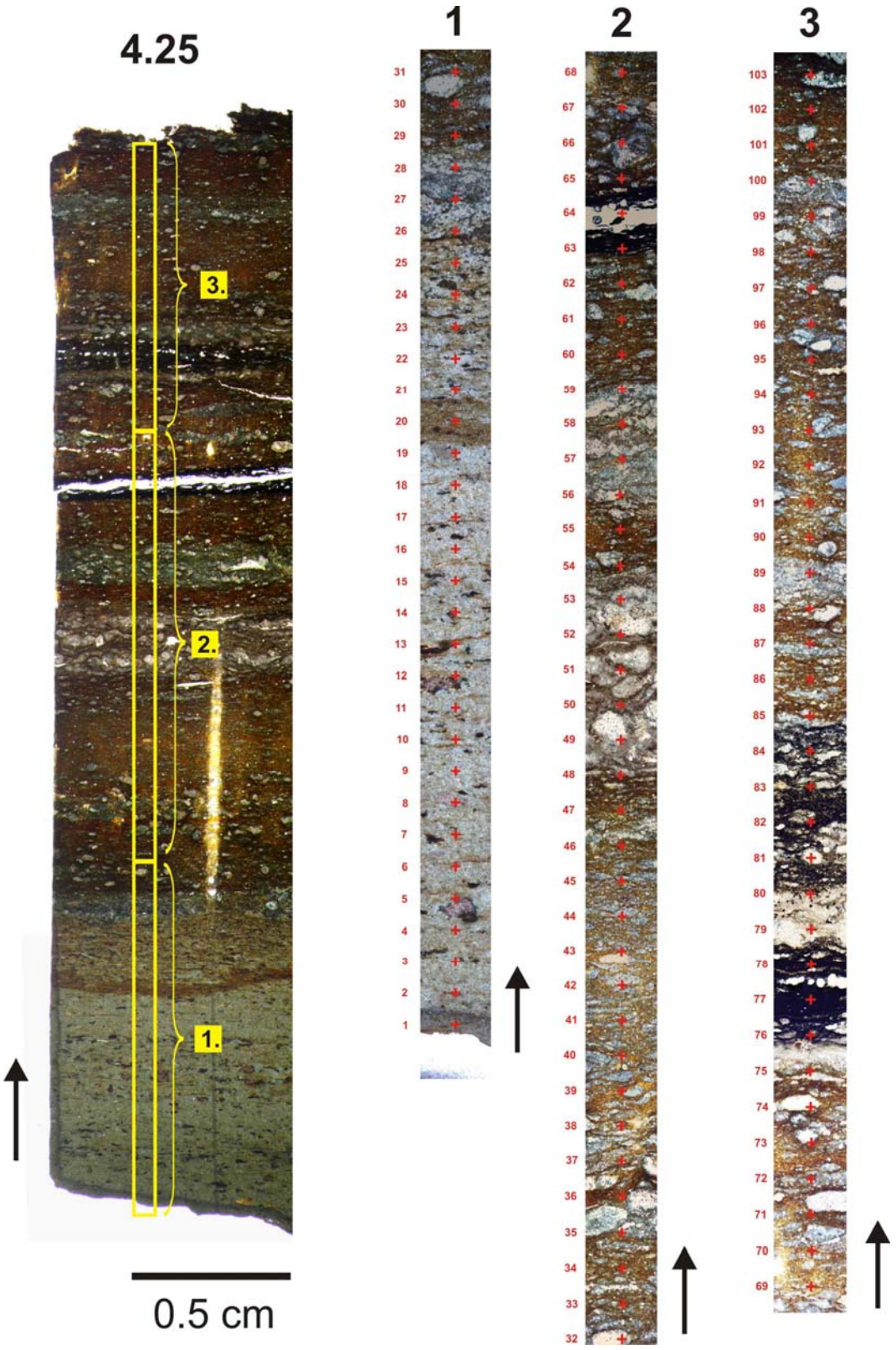

Diagram of peak heigth vs analytical spot number of each of the 8 phases along the Raman scanned section of 4/25 thin section. Intensities are normalized to the highest peak for each spectra. The following Raman bands were used for normalization: rhodochrosite: 1083 cm^{-1}; goethite: 390 cm^{-1}; celadonite: ~551 cm^{-1}; nontronite: ~230 cm^{-1}; quartz: ~463 cm^{-1}; apatite: ~963 cm^{-1}; pyrite: ~380 cm^{-1}; carbonaceous matter: ~1586 cm^{-1}.

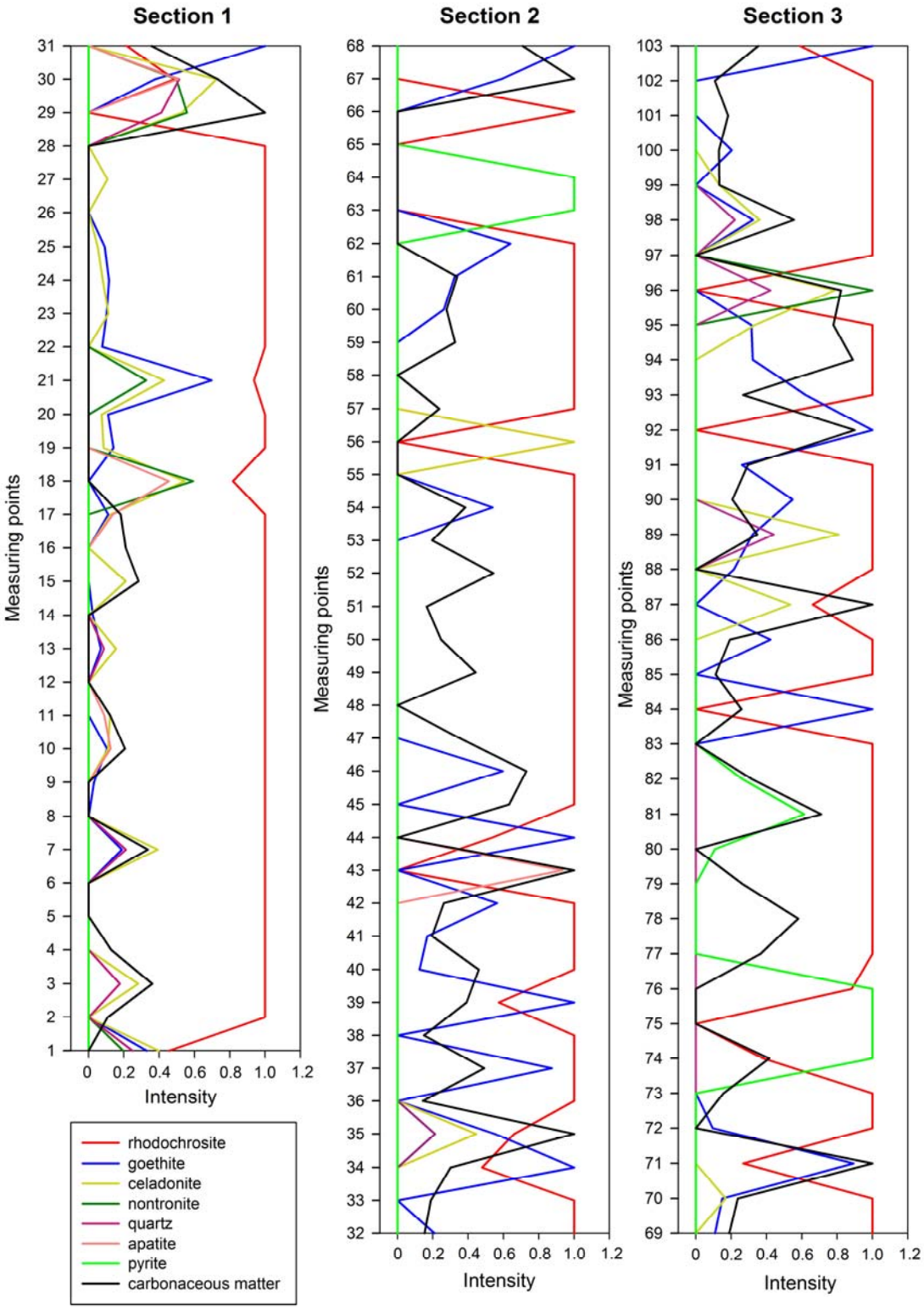

Raman spectra No. 1-20 represent the lower part of the thin section. Mineral abbreviations: apa: apatite; cel: celadonite; gt: goethite; nont: nontronite; qtz: quartz; rds: rodochrosite; car: amorphous carbonaceous matter; epo: epoxy material.

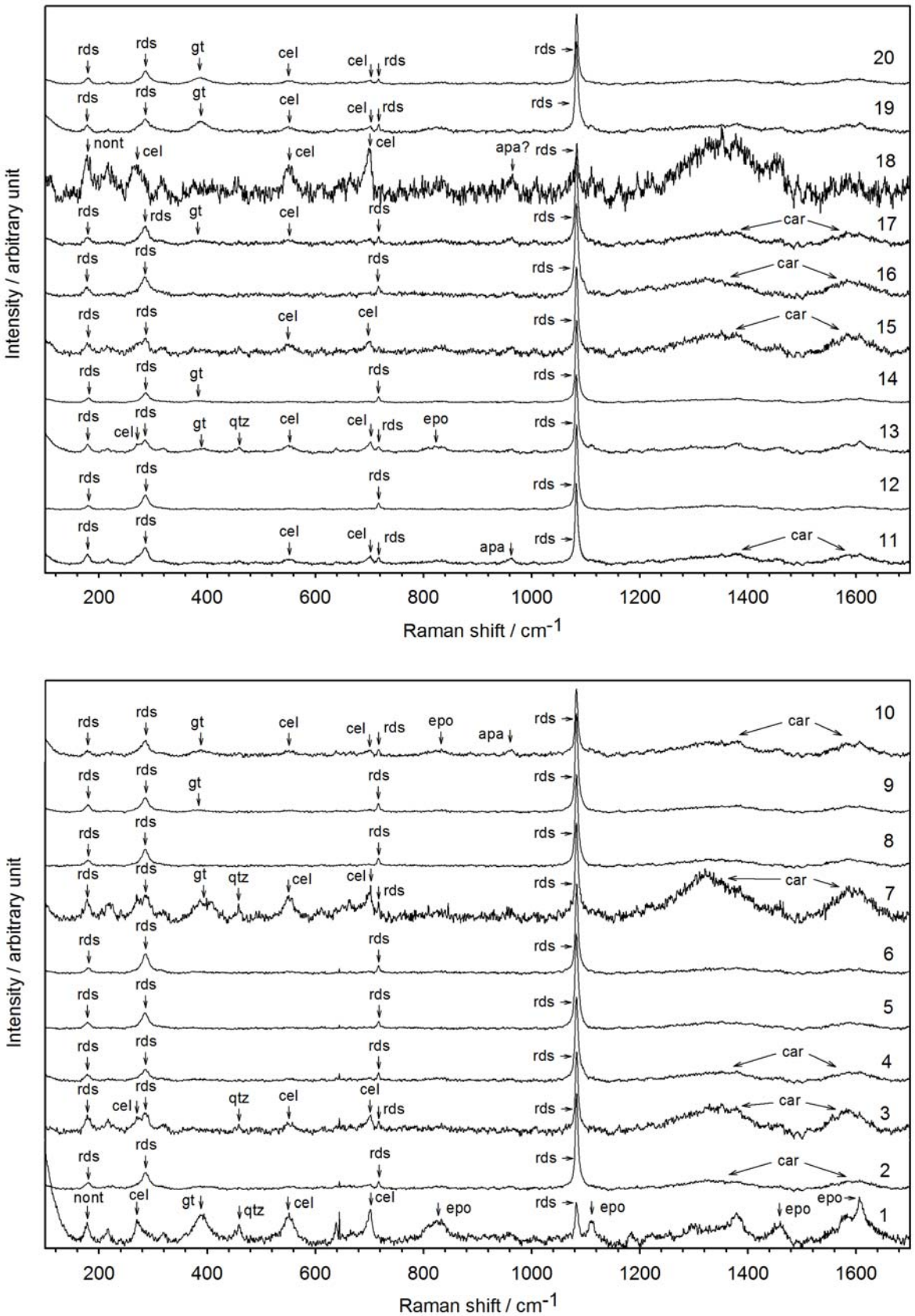

Raman analysis was made on five selected thin sections (4Aa; 4/11/1; 4/19; 4/22; 4/25). Thermo Scientific DXR Raman Microscope was used, with a 532 nm (green) diode pumped solid-state (DPSS) laser with a Nd-YAG source crystal. Measurements were made with 1mW laser power, 50x objective lens in confocal mode (aperture 25 μm pinhole). Acquisition time was 10 min and spectral resolution was ~2 cm^{-1} at each measurement (Szeged University, Hungary)

Fig. DR5. Intensity line profiles (SEM-EDS) of Mn, Si, Fe, K, Al, Mg, Ca of selected oriented thin sections (1/13-2.6 cm; 3/7-1.95 cm; 4/23-3.5 cm)

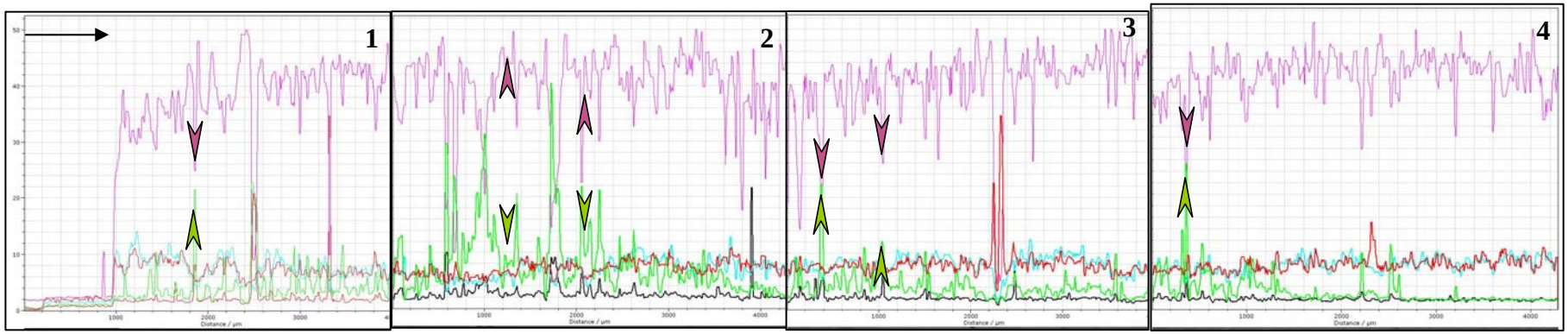

Every part represents 4 mm

Sample 1/13

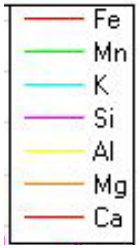

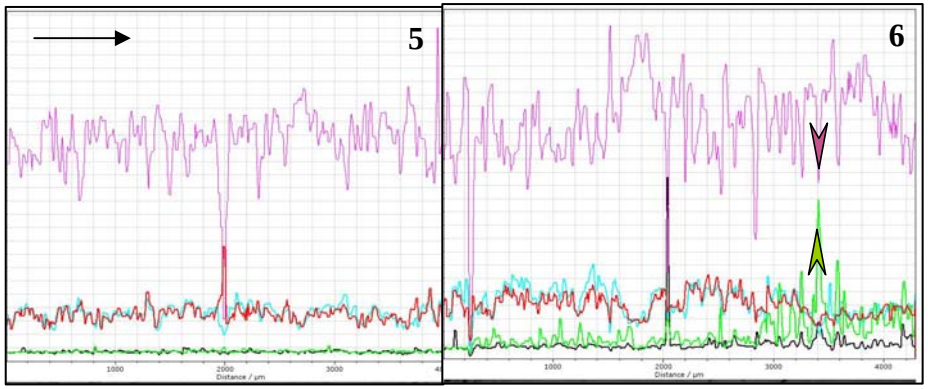

Element distributions were made along line profiles on three selected polished thin sections (1/13, 3/7, 4/23; 24-, 19.2- 35 mm in length; each carbon coated) using a Jeol 25 electron-microprobe with Quantax EDX system, at 25 KV accelerating voltage and 150-360 pA beam current, with scans at 10 µm intervals, for 5 minutes/4 mm length, and intensity profiles of the elements were compared (7200 measurements, three thin sections from bottom, middle, and top of the main ore bed). For Ca, a narrow channel was used and for Fe, Kβ was used for identification to avoid overlap between Mn Kβ and Fe Kα; to get an accurate Fe intensity, a five-times factor was counted on the FeKα/FeKβ ratio). Data were processed by Lomb-type periodicity analysis using a 99% confidence interval. The ore sequence can be regarded as a time series as mineral accumulation took time, laminae represent time. That is why Lomb-type periodicity analysis was used to study possible periodicities. Only significant periods were taken into consideration. This method was also used because it does not need a equidistant time series sequence (Weedon, 2003; Gilgen, 2006). Note that 1/13 is the first ore sample in which Mn enrichment begins; when it occurs, it's rythmicity is the same as other ore samples. To see visually the Fe rythmicity is not so pronounced because the Fe occurs in Fe-rich clay minerals and in goethitic filaments, and the ratio of the two is variable. But in thin sections, the Fe-rich biomat texture is clearly visible. Arrows on the EDS scans were inserted to highlight the opposite rythmicities of Mn and Si at representative places, which helps to follow this rhythmicity across the whole section.

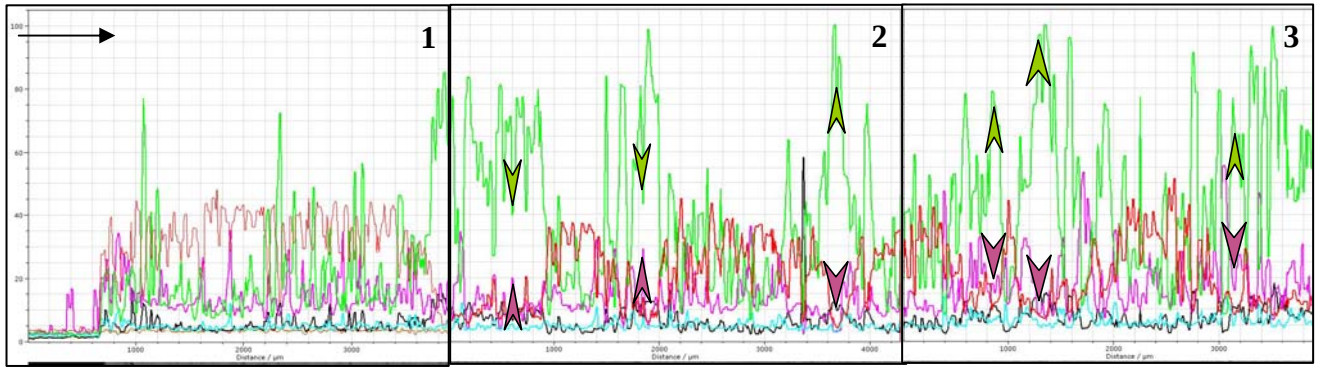

Every part represents 4 mm

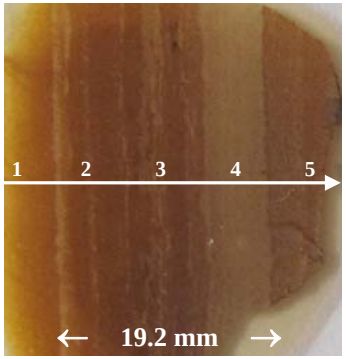

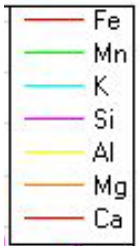

Sample 3/7

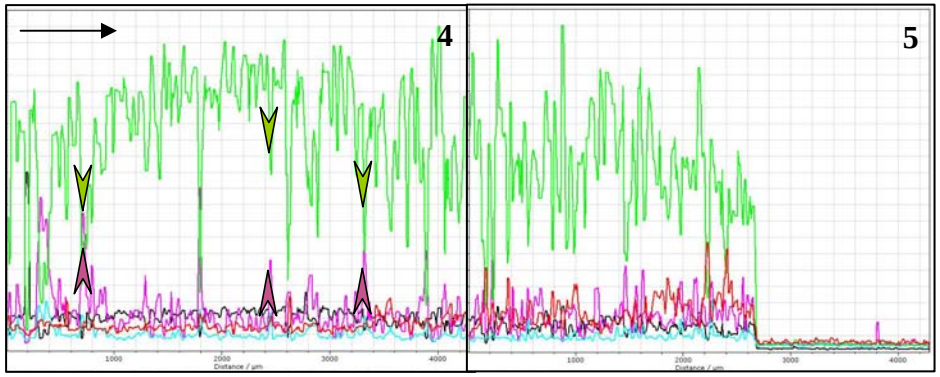

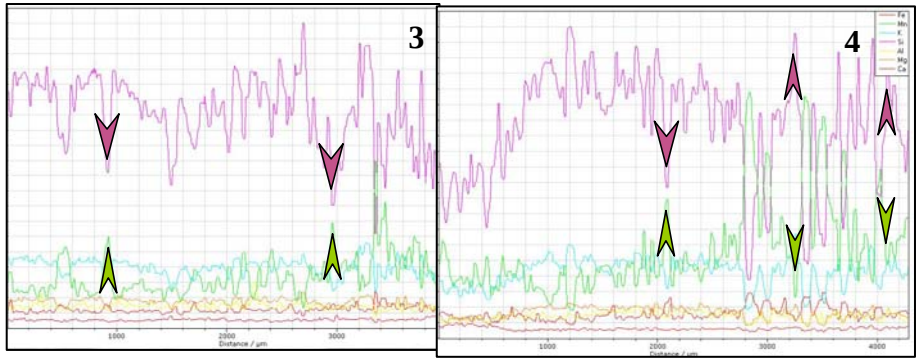

Every part represents 4 mm

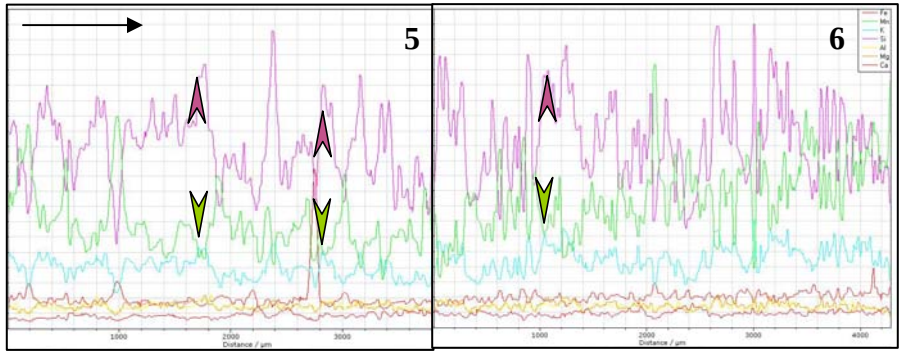

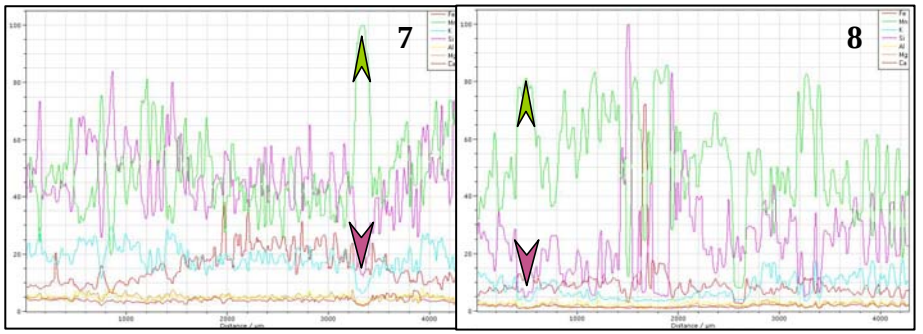

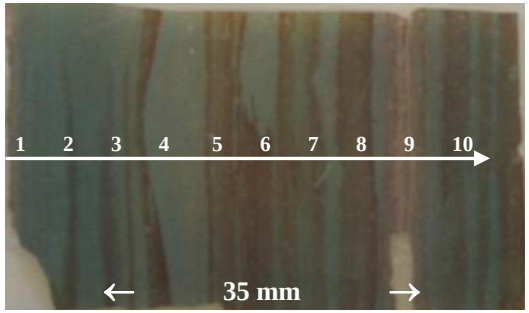

Sample 4/23

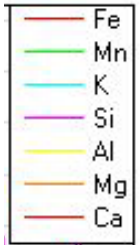

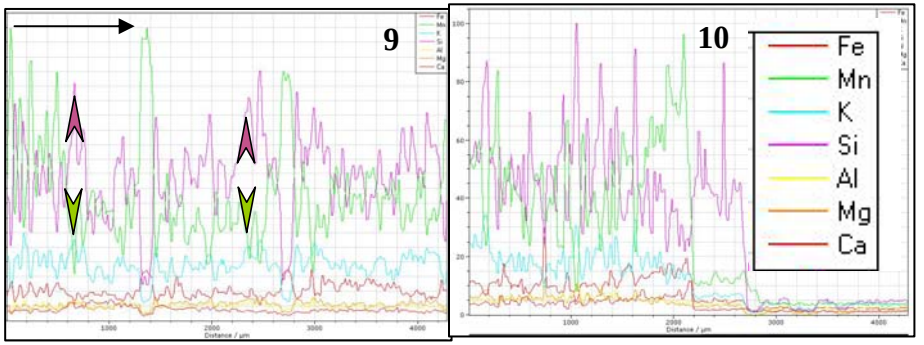

Fig. DR6. Correlation of element intensities (EDS) in samples 1/13, 3/7, 4/23. Sample localities are on Fig. DR1.

Sample 1/13 (number of data for all elements: 1600)

	Fe	Mn	K	Si	Al	Mg
Fe	1					
Mn	-.203**	1				
K	.660**	-.292**	1			
Si	.299**	-.233**	.460**	1		
Al	.309**	-.066**	.460**	.505**	1	
Mg	.507**	-.140**	.711**	.410**	.434**	1

Sample 3/7 (number of data for all elements: 2000)

	Fe	Mn	K	Si	Al	Mg
Fe	1					
Mn	-.463**	1				
K	.105**	.051*	1			
Si	.193**	-.127**	.867**	1		
Al	-.101**	-.012	.325**	,323**	1	
Mg	.128**	-.003	.694**	.827**	,332**	1

Sample 4/23 (number of data for all elements: 3600)

	Fe	Mn	K	Si	Al	Mg
Fe	1					
Mn	.012	1				
K	.433**	-.403**	1			
Si	.155**	-.702**	.835**	1		
Al	.361**	-.555**	.754**	.821**	1	
Mg	.211**	-.630**	.811**	.895**	.879**	1

Key: yellow colour shows correlation between elements with the given significance level; *. Correlation is significant at the 0.05 level (2-tailed); **. Correlation is significant at the 0.01 level (2-tailed).

References Cited

Gilgen, H. 2006, Univariate Time Series in Geosciences: Springer-Verlag Berlin Heidelberg, 718 p.

Weedon, G. 2003, Time-series Analysis and Cyclostratigraphy, Cambridge University Press, 259 p.

http://en.wikipedia.org/wiki/Bacterial_growth